

Deep crustal architecture of the Parnaíba basin of NE Brazil from receiver function analysis: Implications for basin subsidence.

Diogo LOC^{1*}, Jordi Julià¹, Verónica Rodríguez Tribaldos² & Nicky White²

¹*Departamento de Geofísica, Universidade Federal do Rio Grande do Norte, Capim Macio, Natal, CEP 59078-970, Brazil*

²*Bullard Laboratories, Department of Earth Sciences, University of Cambridge, Madingley Rise House, Madingley Road, Cambridge, CB3 0EZ, UK*

*Corresponding author (e-mail: locdiogo@gmail.com)

ABSTRACT

Lithospheric-scale processes, such as the origin and evolution of large cratonic basins, can create big footprints or signatures in the subsurface that can be observed by geophysical means. Our study area is the Parnaíba Basin and the main goal is to provide new images of the crust and lithosphere under the basin and highlight seismic discontinuities. A total of 9 broadband seismographic stations were installed within the PBAP, along an approximately 500 km-long transect across the basin, with interstation spacing of around 50 km. We estimated crustal thickness and Vp/Vs ratio of the Parnaíba Basin by developing P-wave receiver functions. We also developed one-dimensional S-velocity models calculated from the joint inversion of P-wave receiver function and Rayleigh dispersion curves. Results from HK-Stacking, receiver function migration and joint inversion indicate that the Moho dips gently toward the depocenter of the basin (>42 km) and, in the eastern part, some mid-crust reflections at 15-20 km depth, indicating the presence of a mid-crust discontinuity bounding the Borborema Province. We have provided seismic evidence to discriminate the basement beneath of the Parnaíba basin into two blocks, Parnaíba and Teresina blocks, according to the S-velocity models and the cross-section of a migrated P-wave receiver functions across the basin.

Keywords: Broadband Seismology, Parnaíba Basin, Crustal Architecture

The genesis and evolution of large intracratonic basins is an important geological issue that still not completely understood. The basin-forming mechanism and tectonical history of these basins has been much debated with no clear consensus emerging, because there are a varied mechanisms that leading to subsidence of the basin. The Parnaíba basin is one of three large Phanerozoic sedimentary basins in northern South America. This basin is surrounded by three larges cratonic areas, Amazonian, São Luís and São Francisco [Almeida et al. (1981); Brito Neves and Fuck (2013); Cordani et al. (2013)]. The Parnaíba basin is a large, sag-type cratonic basin with a saucer and roughly circular shape and its depocenter reaches up to 3.5 km thick [Góes and Feijó (1994), VAZ (2007) and Daly et al. (2014)].

Recently, Fuck et al. (2008) show that the Precambrian basement of the Parnaíba Basin is composed of several crustal segments, which are the result of agglutination of the existing cratonic fragments (Amazonian, São Luís/West Africa and São Francisco/Congo).

Brito Neves et al. (1984) proposed the existence of a distinct but unexposed basement block beneath the center western part of the basin, trapped between the Amazonian craton and the Borborema orogenic belt, based in regional geology and isotope studies. Currently, de Castro et al. (2014) and de Castro et al. (2016) used a large geophysical data set, involving airborne potential field, seismic and well log data, to reveal the basement inlier block. After this, the authors subdivided the Parnaíba Block into the Parnaíba and Teresina blocks. Follow the same idea, Daly et al. (2014) described the Parnaíba Block with a large deep seismic profile and shed light on the important role of the two major igneous events in the basin development, with extensive extrusives in the Early Jurassic and widespread dykes and sills of Early Cretaceous age.

Knowledge of the crustal thickness is important for understanding the tectonic complexity of the basement. Thus, Moho relief of the South America was studied to several authors in the course of time, like Feng et al. (2004), Feng et al. (2007), Lloyd et al. (2010), van der Meijde et al. (2013), Assumpção et al. (2013b) and Assumpção et al. (2013a). In this paper we characterize the crustal structure beneath the Parnaíba basin by mapping subsurface seismic discontinuities with teleseismic P-wave receiver functions, as proposed by Langston (1979). The data set acquired in 9 seismographic stations, as showed in Figure 1 and Table 1, is part of the Parnaíba Basin Analysis Project (PBAP), a collaboration among several universities and BP Energy do Brasil. We present estimates of the crustal thickness and Vp/Vs ratio at each station obtained through the H- κ stacking procedure of Zhu and Kanamori (2000), as well as S-velocity models obtained by joint inversion between observed receiver functions and surface-wave dispersion velocities from Feng et al. (2007), with the inversion scheme of Julià et al. (2000). We used the common conversion point (CCP) technique, proposed by Frassetto et al. (2010), to produce a 2D cross-section for imaging seismic discontinuities beneath the basin.

Our results confirm previous findings of de Castro et al. (2014) that the Parnaíba Basin basement are divided in Parnaíba and Teresina blocks. Results from H- κ stacking, receiver function migration and joint inversion indicate the Moho dips gently toward the depocenter of the basin, displaying up to three different behaviors: A flat Moho in the depocenter of the basin, which showed the thickest crust (>42 km) and Vp/Vs ratio values around 1,76; A thinning crust towards the eastern flank (<38 km), bounding with the Borborema Province, with Vp/Vs ratio of 1,73, which coincides with the low topographies; An almost flat Moho with thickness of 40 km and Vp/Vs ratio around 1,75 on the western border, bounding with the Araguaia Belt. We also noted a mid-crust reflections at 15-20 km depth, in the eastern part of the basin, indicating the presence of a mid-crust discontinuity. The mid-crust reveals that the Teresina block is a part of the Borborema Province covered by the sediments of the Parnaíba basin and the Parnaíba block is a cratonic fragment, according to features displayed in the S-velocity model and in the cross-section of receiver function migration.

GEOLOGICAL BACKGROUND

de Castro et al. (2016) call attention to shear zones as probable main protagonist in the evolution of the Parnaíba basin. This basin is encircled by sutures zones associated with cratonic blocks collisions, as presented by Daly et al. (2014), de Castro et al. (2014) and de Castro et al. (2016), as shown in the Figure 1. On the eastern side of the basin, the Araguaia suture zone represents the final Neoproterozoic collision between the Amazonian

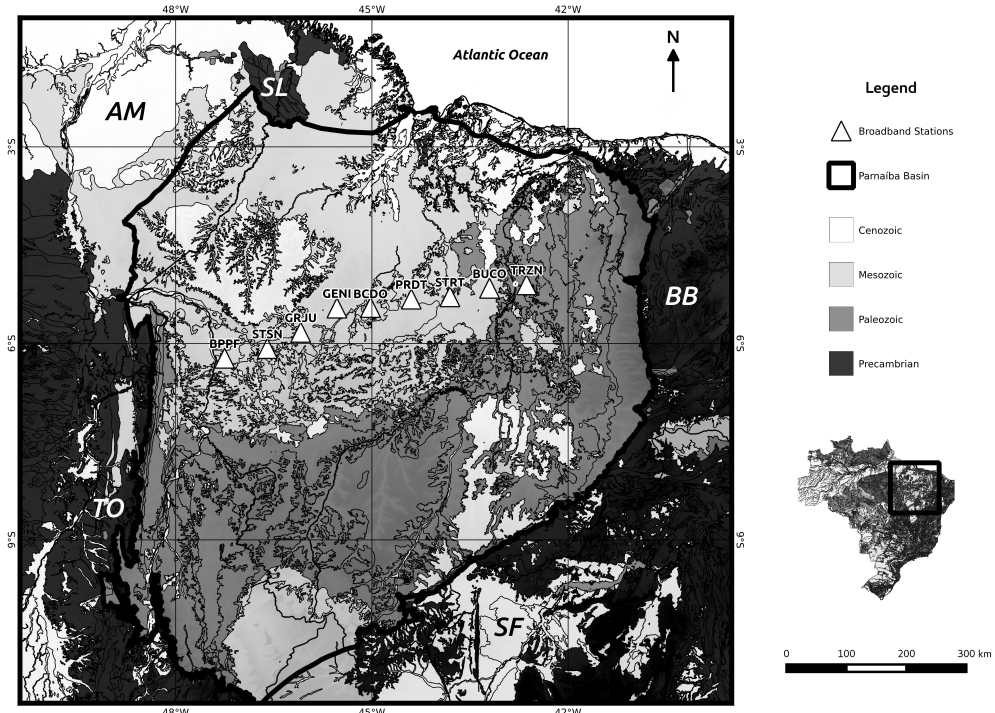


Figure 1: Geological Map with the location of PBAP project stations. AM, Amazonian Craton; BB, Borborema Province; SF, São Francisco Craton; SL, São Luís Craton; TO, Tocantins Province.

craton and the pre-Neoproterozoic Parnaíba block [Fuck et al. (2008), Brito Neves and Fuck (2014)]. On the eastern side of the basin, the Transbrasiliano Lineament, a continental-scale discontinuity characterized by strong magnetic anomalies and by low S wave velocities in the mantle [Fairhead and Maus (2003); Feng et al. (2004); Brito Neves and Fuck (2014)], controls the internal rift geometry and form a 150 km wide rift zone. On the septentrional boundary, the Gurupi Belt represents the deformation zone between the Parnaíba block and São Luís craton. This belt is a sequence of Paleoproterozoic rock assemblages reworked in the Neoproterozoic during a Brasiliano phase (Klein et al., 2005). These lineaments also form Precambrian lithospheric-scale boundaries that were identified in a deep crustal seismic reflection profile across the Parnaíba basin Daly et al. (2014) and represent the collisional sutures of the Amazonian and the São Francisco cratons de Castro et al. (2014).

The basement beneath the Parnaíba basin was subdivided into 2 crustal blocks, Parnaíba and Teresina, by de Castro et al. (2016), in accordance with their magnetic and gravity signatures. The Teresina block shows a high-amplitude reflexion called by Daly et al. (2014) as mid-crustal reflectivity (MCR). This discontinuity is defined as a subhorizontal, curved feature up to 3 km thick terminate into the acoustically featureless Parnaíba block. Daly et al. (2014) show that below this mid-crustal zone are a series of subhorizontal, moderate amplitude events, the base of which appears to define a Moho locally at about 38 km depth. This value supports results found by de Castro et al. (2014) and de Castro et al. (2016). As said by Fuck et al. (2008), de Castro et al. (2014) and de Castro et al. (2016), the Parnaíba Block represents an old continental fragment over a relatively thickened crust, around 42

km, in relation to surrounding crustal zones and its existence has been proposed on the basis of geophysical evidence in addition to petrography and geochronology of the basement rocks.

The evolution of the Parnaíba basin involved five primary tectono-sedimentary sequences and two magmatic pulses. The present-day sag basin consists of at least four tectono-sedimentary sequences separated by regional unconformities, comprising a distinct deposition history [Góes and Feijó (1994), VAZ (2007)]. The basin has an asymmetric geometry, as can be seen in Daly et al. (2014), a elevated western margin and an eastern margin dipping gently. According to Góes and Feijó (1994) the Parnaíba basin depositional history spans the early Paleozoic to the Mesozoic, as seen in 1. The basin is composed of thick, primarily siliciclastic, epicontinental sequences, not to mention Cenozoic alluvial and aeolian deposits.

DATASET

Our dataset is composed by 8 stations using three-component Meridian Compact Posthole sensor and one station using three-component Guralp sensor that compound the PBAP (Parnaíba Basin Analysis Project), a collaboration among several universities in the world and BP Energy do Brasil. These seismic stations are localized in the Northeast of Brazil forming a transect with 600 km width and a interstation spacing of 50 to 70 km, as seen in the Figure 1. The majority of the stations has a deployment from March 2016 to current time. In this work we .In the Table 1 we can found the location and the recording time of each station.

METHODOLOGY

Teleseismic body waveforms recorded at a three-component seismic station contain information on the earthquake source, the earth structure in the vicinity of both source and the receiver, and mantle propagation effects [Langston (1979) ,Ammon (1991), Cassidy (1992), Ligorría and Ammon (1999)]. The receiver function is obtained by removing the effects of source and mantle path by way of the deconvolution of the vertical components from the corresponding horizontal components, therefore isolating the earth structure neighbouring the receiver (Ligorría and Ammon, 1999). The incident P wave energy from teleseismic events will be converted to S wave (Ps) after the interaction with subsurface discontinuities and arrive at the station within the P wave coda after the direct P wave. The analysis of the amplitudes and traveltimes of the interaction phases provides important constraints on the seismic structure under the station (Zhu and Kanamori, 2000).

We have selected teleseismic P-waveforms recorded by the PBAP project stations shown in Figure 1. These stations have sources with epicentral distance raging between 30 and 90 and body wave magnitudes above 5.5 mb. The stations coordinates and recording times for the PBAP project considered in this study are listed in Table 1. To compute the receiver functions, both radial and transverse, we applied the same methodology of Julia et al. (2008) and Luz et al. (2015), utilising a Gaussian filters of the 2.5.

To estimate the crustal thickness and Vp/Vs ratio from the receiver functions we utilise the H- κ stacking technique of Zhu and Kanamori (2000). This procedure performs a grid-search over a stacking surface built by summing a weighted combination of the Ps, PpPs

Table 1: Station coordinates and recording time window from Parnaíba basin.

Station	Latitude	Longitude	Recording time
BPPF	-6.2271	-47.2518	2016.188 – 2016.345
BUCO	-5.1586	-43.2010	2016.118 – 2016.344
GENI	-5.4612	-45.5344	2016.105 – 2016.346
GRJU	-5.8308	-46.0882	2016.104 – 2016.345
PRDT	-5.3241	-44.3974	2016.106 – 2016.344
STSN	-6.0787	-46.5986	2016.105 – 2016.345
STSР	-5.2889	-43.8063	2016.119 – 2016.344
TRSN	-5.1056	-42.6344	2016.118 – 2016.344
BCDO	-5.4517	-45.0203	2015.222 – 2016.293

and PpSs+PsPs amplitudes. In this procedure, the P-wave velocity for the layer, average of 6.3 km/s to the basin, and the phase weights must be specified a priori, as shown in Table 2. Confidence bounds for the thickness and Vp/Vs estimates have been obtained by bootstrapping, as explained in Efron and Tibshirani (1991), the receiver function waveforms at each station with 200 replications. Luz et al. (2015) have a detailed explain about this procedure.

S-wave velocity models beneath PBAP stations in the Parnaíba basin have been obtained through the inversion scheme of Julià et al. (2000). To ensure that both data sets sample similar regions of the Earth, we identified the surface-wave tomographic cell enclosing each station in our study and extracted the local group velocity curve for the tomographic cell. We then inverted the receiver functions jointly with the extracted dispersion curve, in this case, dispersion curves from Feng et al. (2007). The data sets were normalized for the different number of data points and physical units prior to inversion. The procedure includes an influence factor equal to 0.5 that weights the contribution of each data and to provide a good compromise between fitting the receiver functions and the dispersion velocities. The starting model for the linearized procedure is the 1D velocity model measured by Almeida et al. (2015). Some instabilities that drive the iterative process away from convergence was overcome through smoothness constraints in the velocity profiles, at the expense of losing resolution in the inverted models. Usually, a total of 9 iterations sufficed for the inversion process to converge to a final S-velocity model.

The final step in our analysis was the migration and stacking of P-wave receiver functions for the PBAP project seismic. We followed the same approach as in Almeida et al. (2015), which one investigated the crustal architecture across the Borborema Province. In total, our expanded dataset includes 744 receiver function waveforms throughout the basin. To stack the receiver function waveforms we utilized the common conversion point (CCP) migration and stacking procedure of Frassetto et al. (2010). The procedure combines the CCP stacking of Gilbert and Sheehan (2004) with the phase-weighting scheme of Schimmel and Paulssen (1997) to enhance coherent P-to-S conversions in the stacks. A detailed explain about this procedure can be found in Frassetto and Thybo (2013) and Almeida et al. (2015).

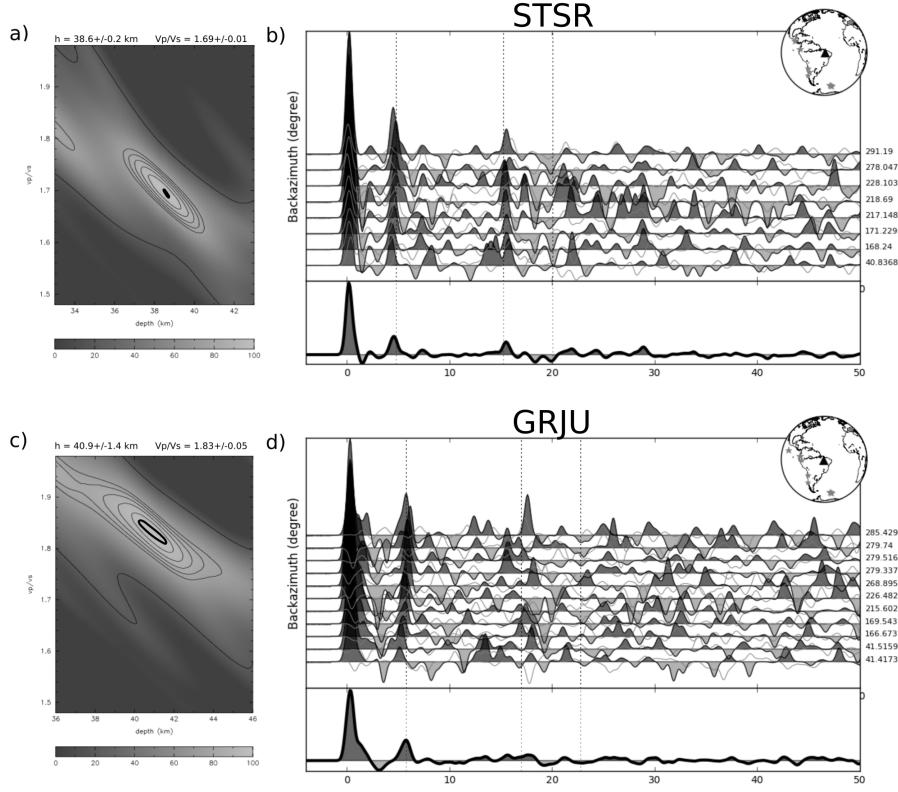


Figure 2: Moaisc showing $H\text{-}\kappa$ stacking results for GRJU (top) and STSR (bottom) stations. For each station the top panels display the receiver function, radial (black lines) and tranverse (red lines), sorted by backazimuth and the map with the location of the earthquakes utilised (yellow stars). The bottom panels display the receiver function stacked with the Ps , $PpPs$, and $PpSs+PsPs$ phases times superimposed to the receiver functions and a figure showing the $H\text{-}\kappa$ stacking screen.

RESULTS

Analising the results displayed in the Figure 2, we can see the radial and transverse receiver functions selected for the GRJU and TRSN stations. A simple inspection of the waveforms reveals important properties of the propagating medium beneath each station. Comparing the amplitude of the transverse (red lines) and radial (black lines) receiver functions for both stations, we observe that the transverse receiver functions generally display small amplitudes compared to the corresponding radial waveforms. For a laterally homogeneous media is expected a transverse receiver function have an amplitude equal to zero. In the Figure 2 we see small transverse amplitudes indicating that the medium under the GRJU station can be approximate as laterally homogeneous and isotropic. Moreover, in the TRSN station the amplitude of the tranverse component is higher than the GRJU station, thus the medium beneath this station is different of the GRJU station, and we need some precaution in our estimate. Also, we can identify the signature of the sedimentary cover, negative peak, in all the radial waveforms in both stations. The shift in the main peak, for instance, is due to a large Ps phase generated at the sediment – bedrock interface that arrives shortly after the

incoming P-wave, and cannot be resolved by the Gaussian filter (Cassidy, 1992). Also other apparent peaks and troughs between 1 and 3 s are also caused by the interaction of the impinging P-wavefront with sedimentary structure. Finally, the Ps phase generated at the Moho is generally apparent in all the waveforms at about 5 s, but the multiply reverberated phases in the bulk crustal structure are generally harder to identify. The wavelengths of the reverberated phases are shorter than those of the Ps phase, and a gradational crust–mantle boundary could reduce their amplitudes significantly (Julià et al., 2000). Some multiples are hard to detect in the waveforms, especially the PpSs+PsPs phase, Figure 2, and this variability is translated into large confidence bounds during the bootstrap resampling (Julia et al., 2008). We can see a backazimuth dependence of the receiver function in the top panel of the Figure 2, but this problem is not a problem because our earthquakes have a restrict backazimuth window.

Table 2: *H- κ stacking parameters and results from Parnaíba basin.*

Station	n	Vp	w1	w2	w3	h0	H(km)	Vp/Vs
BPPF	5	6.3	0.4	0.4	0.2	41	41.20 ± 3.857	1.750 ± 0.075
BUCO	11	6.3	0.4	0.3	0.3	40	38.00 ± 1.33	1.735 ± 0.033
GENI	7	6.3	0.4	0.3	0.3	44	44.00 ± 2.05	1.766 ± 0.088
GRJU	11	6.3	0.4	0.3	0.3	40	41.00 ± 1.41	1.827 ± 0.047
PRDT	11	6.3	0.4	0.3	0.3	40	38.70 ± 3.36	1.815 ± 0.081
STSN	12	6.3	0.4	0.3	0.3	40	40.50 ± 1.56	1.751 ± 0.043
STSR	8	6.3	0.4	0.3	0.3	40	38.59 ± 0.23	1.693 ± 0.011
TRSN	12	6.3	0.4	0.3	0.3	40	38.00 ± 2.26	1.751 ± 0.052
BCDO	3	6.3	0.4	0.3	0.3	40	40.00 ± 3.34	1.700 ± 0.081

* The table includes the number of waveforms (n), P-wave velocity assumed (Vp), weights for the Ps (w1), PpPs (w2), and PpSs + PsPs (w3) phases.

Table 2 lists the H- κ stacking results for the PBAP stations in the Parnaíba basin. The crustal thicknesses range between 38 and 44 km and are generally constrained within 3 km. Overall, these values are in excellent agreement with the estimates from previous continental scale studies, as Feng et al. (2007), Lloyd et al. (2010) and Assumpção et al. (2013a). Results from HK-Stacking, receiver function migration and joint inversion indicate the Moho dips gently toward the depocenter of the basin, nearby the GRJU station, displaying up to three different behaviors: A flat Moho in the depocenter of the basin, which showed the thickest crust. A thinning crust towards the eastern flank, bounding with the Borborema Province, as can be observed in the S-velocity models in the Figure 3 and in the CCP migration cross-section in the bottom of the Figure 4. We can see a consonance among the crustal thickness nearby the Borborema Province calculated by our data and by the studies of Pavão et al. (2013), Almeida et al. (2015) and Luz et al. (2015). We have a lack of works in seismology in the western part, but we can find some analogous results in de Castro et al. (2014) and Daly et al. (2014), notwithstanding our estimates recover a thickest crust comparing with these authors.

Studying the variation of Vp/Vs ratio on grounds of the complexity of the crust composition should provide important constraints of the geological history. Although, the Vp/Vs values are more variable and less tightly constrained (Julia et al., 2008). Comparing the Vp/Vs ratio of the Table 2, we can see that the bulk composition of the eastern part of the basin, close-by 1.73, is more felsic compared to western part, around 1.76, according to Christensen (1996) classification. Chevrot and van der Hilst (2000) mention that the Vp/Vs

ratio varies as a function of crustal thickness inside a geological province. Table 2 indicates an increment of Vp/Vs ratio with increasing crustal thickness, as well as in the bottom panel of the Figure 4. GRJU station shows a Vp/Vs of 1.827 ± 0.047 , this can be explained due to the increase of the thickness, concomitantly growth the mafic lower crust (granulite composition), thus, according to Christensen (1996), is expected high values of Vp/Vs, as we can check in the stations in the western part of the basin. Similarly, Christensen (1996) and Julia et al. (2008) suggest that high values can be related with a mafic crust or a concentration of basaltic rocks, correlating with gross thickness of diabase intrusions in the center of the basin (Daly et al., 2014), as observed in the Vp/Vs ratio for the PRDT station.

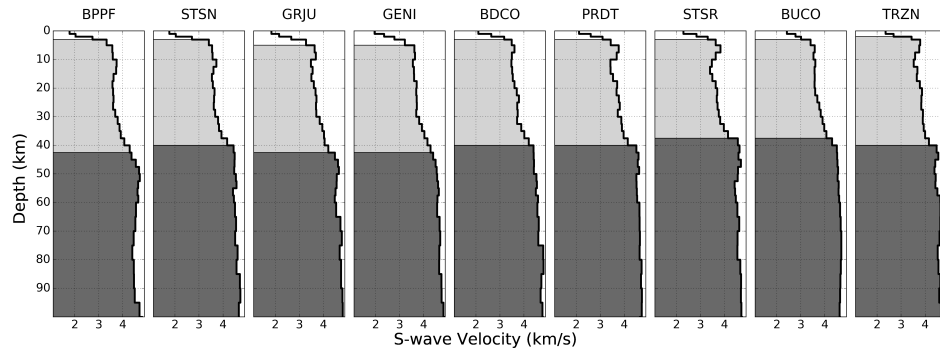


Figure 3: *Joint inversion models for each station sorted according the station location in the Figure 1. Colors represent S-wave velocities: The sedimentary layer, > 3.3 km/s (white); crust, between 3.3 to 4.3 km/s (gray); and mantle, < 4.3 km/s (dark gray). These values are based in models calculated from Mooney et al. (1998).*

Joint inversion models in the Figure 3 reveal two different structural patterns according to our interpretation, shown in the lower panel. First of all, we can differentiate in the top of each model a sedimentary layer, characterized by low velocities (blue color). We do not insert a priori information about a sedimentary layer in the start model, as seen in the start model of Almeida et al. (2015), thus the inversion been able to recover the sedimentary structure correctly, mainly the thickness of the basin ($> 4\text{km}$). The analyzed stations data in the Teresina Block (PRDT, STRT, BUCO and TRSN) allow us to interpret a mid-crust discontinuity depth between 15 km and 25 km. This discontinuity is indicated by a high velocity layer (red color), but we cannot identify this discontinuity in the western part, as shown by Daly et al. (2014). The mid-crust discontinuity is called by Pavão et al. (2013) as upper-lower crust discontinuity, latterly interpreted as detachment zone by Almeida et al. (2015). Teresina Block shows a crustal compartmentation, with a Moho discontinuity well-identified (sharp discontinuity), however, Parnaíba Block exhibits a diffuse Moho, probably a gradational boundary. In the Parnaíba Block is not observed a mid-crust discontinuity, or a clearly segmentation of the crust, as can be observed in the Figure 3. The thicknesses from the inverted models, as expected, are in good agreement with the thicknesses calculated from H- κ stacking, Table 2. The high velocity nearby to 5 km of depth can be related with some basaltic intrusions ou mafic bodies, or is just an artefact created due to lack of a priori information about the sedimentary layer.

The migrated cross-section, Figure 4, obtained through the receiver function CCP stacks indicates that the crustal basement of the Parnaíba Basin can be divided into two blocks,

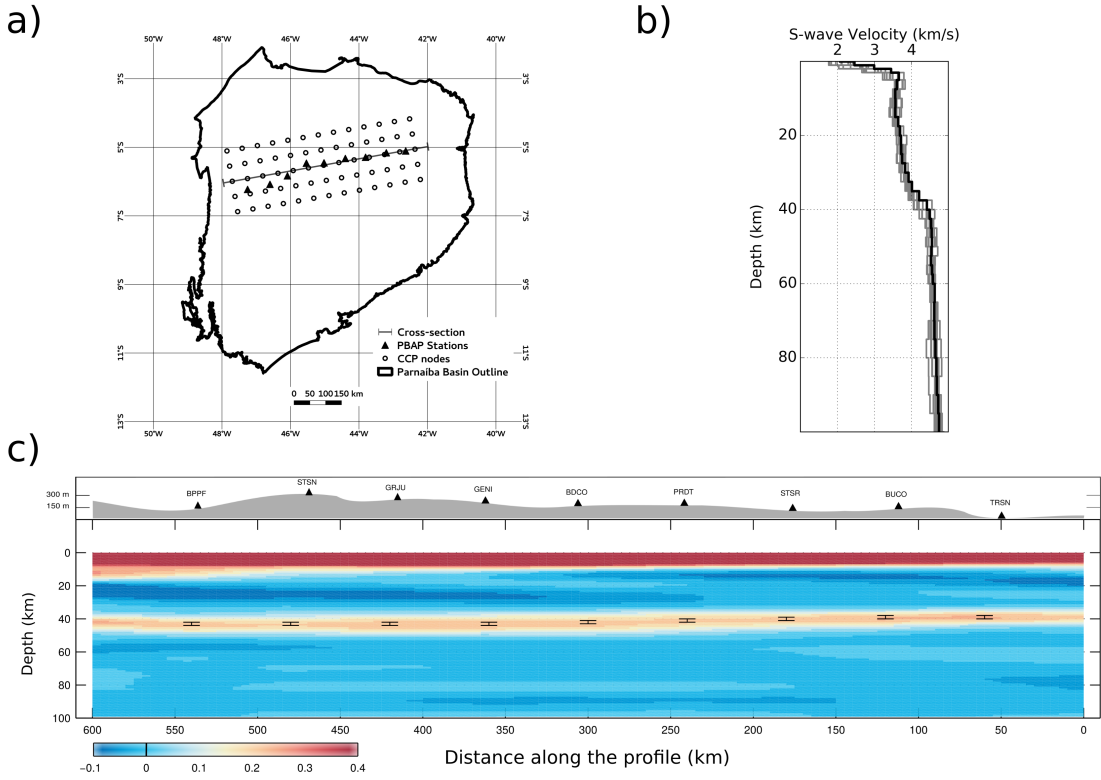


Figure 4: Cross-section corresponding to profile in Figure . In the top of the panel we can see the topography and the seismic stations (black triangles), and the low panel displays color-coded receiver function stacked amplitudes. Red colors indicate positive amplitudes (i.e., positive velocity contrast), while blue colors indicate negative amplitudes (i.e., negative velocity contrast). The black segments mark the location of the Moho P_s conversion at the crust–mantle boundary from bootstrapping.

equivalently to the S-velocity model results. The separation between the western and eastern side is evident, due to the structural pattern of each block. The major discontinuities detected in the cross-section is at 15–25 km and at 38–44 km depth, mid-crustal and Moho discontinuity, respectively. Both discontinuities present a gently slope, but they dips in opposite directions, as seen in the lower panel of the Figure 4. Moho dips gently toward the depocenter of the basin, meanwhile the mid-crust discontinuity dips toward the Borborema Province. Published results of crustal structure for the Parnaíba Basin, de Castro et al. (2014) and Daly et al. (2014), identify a deeper crust–mantle boundary, as well as our $H\kappa$ stacking and Joint Inversion results. Daly et al. (2014) recognise the shallower anastomosing discontinuity, but just locally. de Castro et al. (2014) create a interpretative model for airborne gravity and magnetic data of the Parnaíba Basin, and divided the basement into upper, middle and lower crust segments. Another interesting relation can be observed within the Parnaíba Basin, the Figure 4 reveals that the eastern side, regions of low topography, is characterized by a thin crust (38 km), while regions of elevated topography, current depocenter, tend to display a crust of 41 km or thicker. This behavior is controversial,

because is intuitive that the current depocenter needs to be the lowest part of the basin. Additionally, Almeida et al. (2015) report the same behavior within the Borborema Province.

TECTONIC IMPLICATIONS

The most important finding in our study is the capability to divide the Parnaíba Basin basement into two blocks using passive-source seismology, following the statement proposed by de Castro et al. (2014). The presence of an intra-crustal discontinuity at about 10–25 km depth within the Teresina Block can be related with a buried part of the Borborema Province covered by sediments of the Parnaíba Basin, because both Pavão et al. (2013) and Almeida et al. (2015) reported this same discontinuity in the Borborema Province. Almeida et al. (2015) interpreted this discontinuity as a detachment zone that resulted from Mesozoic extension, and proposed that it might be connected with a widespread network of shear-zones, which would in turn have helped accommodate extension within the brittle upper crust. But, to confirm this statement we need stations covering regions along the Brasiliano Lineament, because if this lineament affect this reflection pattern, this structures are older than Mesozoic age.

Previously, Daly et al. (2014) reported the Parnaíba block as a "seismically transparent block", but, fortunately, we could calculate Moho thickness with a good precision. Moreover, we cannot identify some internal structures in this block. We interpreted, as well as Fuck et al. (2008), Brito Neves and Fuck (2014) and Assumpção et al. (2013a), that the Parnaíba Block is an old cratonic fragment. Analysing the internal structure of Parnaíba block through receiver functions is hard because the velocity contrast is not so high and some mineral phase changes are transitional, as we can see in the work of Assumpção et al. (2002). Thus, we are not able to illuminate the internal structure.

CONCLUSIONS

We have provided seismic evidence of the subdivision of the block beneath of the Parnaíba basin. Our results are consistent with the interpretation of de Castro et al. (2014), which postulated that the Parnaíba Basin basement are divided in Parnaíba and Teresina blocks according the S-velocity models and cross-section of a migrated P-wave receiver functions. Summarizing, we have obtained 9 point estimates of crustal thickness and bulk V_p/V_s ratio across the Parnaíba basin of NE Brazil. S-velocity models and cross-section of a migrated P-wave receiver functions in the Parnaíba Basin have demonstrated the existence of two main seismic discontinuities characterizing the crustal architecture of the basin. The deeper discontinuity displays values ranging between 38 and 44 km, and has been identified with the crust–mantle boundary; the shallower discontinuity occurs at depths of 15–25 km and preferentially within western part of the basin, region of thin crust, which coincides with the low topographies.

REFERENCES

- Almeida, F. F. M., Y. Hasui, B. B. Brito Neves, and R. A. Fuck, 1981, Brazilian structural provinces: An introduction: **17**, 1–29.

- Almeida, Y. B., J. Julià, and A. Frassetto, 2015, Crustal architecture of the borborema province, NE brazil, from receiver function CCP stacks: Implications for mesozoic stretching and cenozoic uplift: **649**, 68–80.
- Ammon, C. J., 1991, The isolation of receiver effects from teleseismic p waveforms: **81**, 2504–2510.
- Assumpção, M., M. Bianchi, J. Julià, F. L. Dias, G. Sand França, R. Nascimento, S. Drouet, C. G. Pavão, D. F. Albuquerque, and A. E. V. Lopes, 2013a, Crustal thickness map of brazil: Data compilation and main features: **43**, 74–85.
- Assumpção, M., M. Feng, A. Tassara, and J. Julià, 2013b, Models of crustal thickness for south america from seismic refraction, receiver functions and surface wave tomography: **609**, 82–96.
- Assumpção, M., D. James, and A. Snoke, 2002, Crustal thicknesses in se brazilian shield by receiver function analysis: Implications for isostatic compensation: **107**.
- Brito Neves, B., R. Fuck, U. Cordani, and A. Thomaz, F., 1984, Influence of basement structures on the evolution of the major sedimentary basins of brazil: A case of tectonic heritage: **1**, 495–510.
- Brito Neves, B. B., and R. A. Fuck, 2013, Neoproterozoic evolution of the basement of the south-american platform: **47**, 72–89.
- Brito Neves, B. B. d. B., and R. A. Fuck, 2014, The basement of the south american platform: Half laurentian (n-NW)+half gondwanan (e-SE) domains: **Complete**, 75–86.
- Cassidy, J. F., 1992, Numerical experiments in broadband receiver function analysis: **82**, 1453–1474.
- Chevrot, S., and R. D. van der Hilst, 2000, The poisson ratio of the australian crust: geological and geophysical implications: Earth and Planetary Science Letters, **183**, 121 – 132.
- Christensen, N. I., 1996, Poisson's ratio and crustal seismology: **101**, 3139–3156.
- Cordani, U. G., M. M. Pimentel, G. d. Araujo, C. Eduardo, and R. A. Fuck, 2013, The significance of the transbrasiliiano-kandi tectonic corridor for the amalgamation of west gondwana: **43**, 583.
- Daly, M. C., V. Andrade, C. A. Barousse, R. Costa, K. McDowell, N. Piggott, and A. J. Poole, 2014, Brasiliano crustal structure and the tectonic setting of the parnaíba basin of NE brazil: Results of a deep seismic reflection profile: **33**, 2014TC003632.
- de Castro, D. L., F. H. Bezerra, R. A. Fuck, and R. M. Vidotti, 2016, Geophysical evidence of pre-sag rifting and post-rifting fault reactivation in the parnaíba basin, brazil: **7**, 529–548.
- de Castro, D. L., R. A. Fuck, J. D. Phillips, R. M. Vidotti, F. H. R. Bezerra, and E. L. Dantas, 2014, Crustal structure beneath the paleozoic parnaíba basin revealed by airborne gravity and magnetic data, brazil: **614**, 128–145.
- Efron, B., and R. Tibshirani, 1991, Statistical data analysis in the computer age: **253**, 390–395.
- Fairhead, J., and S. Maus, 2003, CHAMP satellite and terrestrial magnetic data help define the tectonic model for south america and resolve the lingering problem of the pre-break-up fit of the south atlantic ocean: **22**, 779–783.
- Feng, M., M. Assumpção, and S. Van der Lee, 2004, Group-velocity tomography and lithospheric s-velocity structure of the south american continent: **147**, 315–331.
- Feng, M., S. van der Lee, and M. Assumpção, 2007, Upper mantle structure of south america from joint inversion of waveforms and fundamental mode group velocities of rayleigh waves: **112**, no. B4, B04312.
- Frassetto, A., and H. Thybo, 2013, Receiver function analysis of the crust and upper mantle

- in fennoscandia – isostatic implications: **381**, 234–246.
- Frassetto, A., G. Zandt, H. Gilbert, T. J. Owens, and C. H. Jones, 2010, Improved imaging with phase-weighted common conversion point stacks of receiver functions: **182**, 368–374.
- Fuck, R. A., B. B. Brito Neves, and C. Schobbenhaus, 2008, Rodinia descendants in south america: **160**, 108–126.
- Gilbert, H. J., and A. F. Sheehan, 2004, Images of crustal variations in the intermountain west: **109**, no. B3, B03306.
- Góes, A., and F. Feijó, 1994, Bacia do parnaíba: **8**, 57–67.
- Julia, J., M. Assumpção, and M. P. Rocha, 2008, Deep crustal structure of the parana basin from receiver functions and rayleigh-wave dispersion: Evidence for a fragmented cratonic root: **113**, no. B8.
- Julià, J., C. J. Ammon, R. B. Herrmann, and A. M. Correig, 2000, Joint inversion of receiver function and surface wave dispersion observations: **143**, 99–112.
- Klein, E. L., C. A. V. Moura, R. S. Krymsky, and W. L. Griffin, 2005, The gurupi belt, northern brazil: lithostratigraphy, geochronology, and geodynamic evolution.
- Langston, C. A., 1979, Structure under mount rainier, washington, inferred from teleseismic body waves: **84**, no. B9, 4749–4762.
- Ligorría, J. P., and C. J. Ammon, 1999, Iterative deconvolution and receiver-function estimation: **89**, 1395–1400.
- Lloyd, S., S. van der Lee, G. S. França, M. Assumpção, and M. Feng, 2010, Moho map of south america from receiver functions and surface waves: **115**, no. B11, B11315.
- Luz, R. M. N., J. Julià, and A. F. do Nascimento, 2015, Bulk crustal properties of the borborema province, NE brazil, from p-wave receiver functions: Implications for models of intraplate cenozoic uplift: **644–645**, 81–91.
- Mooney, W. D., G. Laske, and T. G. Masters, 1998, CRUST 5.1: A global crustal model at $5^\circ \times 5^\circ$: **103**, no. B1, 727–747.
- Pavão, C. G., G. S. França, M. Bianchi, T. de Almeida, and M. G. Von Huelsen, 2013, Upper-lower crust thickness of the borborema province, NE brazil, using receiver function: **42**, 242–249.
- Schimmel, M., and H. Paulssen, 1997, Noise reduction and detection of weak, coherent signals through phase-weighted stacks: **130**, 497–505.
- van der Meijde, M., J. Julià, and M. Assumpção, 2013, Gravity derived moho for south america: **609**, 456–467.
- VAZ, P. e. a., 2007, Bacia do parnaíba: **15**, 253–263.
- Zhu, L., and H. Kanamori, 2000, Moho depth variation in southern california from teleseismic receiver functions: **105**, no. B2, 2969–2980.